for similar complexes in which S-bonded ligands are present.[19] The [L] dependence of the data suggests the secondary reaction to be a substitution process, the intercept being due to either the reverse solvolysis step or a parallel dissociative ring-opening reaction of the dien ligand followed by a non-rate-determining substitution step.

To summarize, the principal feature of the reactions involving the nucleic free bases and the nucleosides is that, contrary to normal square-planar substitution, the solvolysis of $Pd(dien)Cl^+$ is not the rate-determining step but the subsequent anation of $Pd(dien)OH_2^{2+}$ is instead. The spontaneous solvolysis preceding the rate-determining anation can, depending on the relative magnitudes of k_1, $k_{-1}[Cl^-]$, and $k_{an}[L]$ (cf. Scheme I), either be treated as a preequilibration (k_1, $k_{-1}[Cl^-] > k_{an}[L]$, eq 3, Figure 4) or a steady-state controlling step (k_1, $k_{-1}[Cl^-] \sim k_{an}[L]$, eq 4, Figure 5), a change-over between the two for a given nucleic moiety being effected by a sufficient change in its concentration. The reverse aquation following the rate-determining anation becomes sufficiently significant in a few cases (Figures 3 and 6) to contribute to the observed rate constant (eq 1 and 6) and competes in the presence of chloride ion with a reaction that probably involves ion pairing (cf. Scheme II). The rate-determining step of the reactions involving the 5′-nucleotides is neither spontaneous solvolysis nor subsequent anation but a secondary substitution that is still to be identified. The mentioned anation, reverse aquation, and other subsequent reactions are expected to play an important role in the intimate mechanism of the interaction of related antitumor complexes with nucleic acid moieties. The approach of various authors, for instance, to slow down the reactions of *cis*-$[Pt(NH_3)_2Cl_2]$ with AMP and GMP by studying them in a large excess of chloride[4e,8c] had been based on the supposition that hydrolysis of *cis*-$[Pt(NH_3)_2Cl_2]$ is the rate-determining step[21] and that this hydrolysis is hampered by high chloride ion concentrations,[2,8a] but we arrived at a different explanation for the retardation in view of our results. Similarly, some other aspects that may contribute to the fundamental understanding of the substitution behavior of related antitumor complexes are being investigated in more detail in our laboratories.

Acknowledgment. The authors gratefully acknowledge financial support from the Deutsche Forschungsgemeinschaft and the Fonds der Chemischen Industrie. E.L.J.B. thanks the Alexander von Humboldt-Stiftung for a fellowship and the South African Council for Scientific and Industrial Research and the Potchefstroom University for Christian Higher Education for sabbatical leave bursaries.

Registry No. A, 73-24-5; C, 71-30-7; G, 73-40-5; I, 68-94-0; T, 65-71-4; U, 66-22-8; AMP, 61-19-8; CMP, 63-37-6; GMP, 85-32-5; IMP, 131-99-7; TMP, 365-07-1; UMP, 58-97-9; $Pd(dien)OH_2^{2+}$, 53773-87-8; $Pd(dien)Cl^+$, 17549-31-4.

(21) Horacek, P.; Drobnik, J. *J. Biochim. Biophys. Acta* **1971**, *254*, 341; Drobnik, J.; Horacek, P. *Chem.-Biol. Interact.* **1973**, *7*, 223.

Contribution from the Department of Chemistry, Florida Atlantic University, Boca Raton, Florida 33431, and Contribution No. 915 from Battelle-Kettering Laboratory, Yellow Springs, Ohio 45387

Two-Electron Transfer Accompanied by Metal–Metal Bond Formation. Synthesis and Electrochemistry of Dinuclear Molybdenum and Tungsten Carbonyl Thiolates

Doris A. Smith,[†] Botao Zhuang,[§] William E. Newton,[‡] John W. McDonald,*[‡] and Franklin A. Schultz*[†]

Received December 23, 1986

The binuclear, thiolate-bridged complexes $[Et_4N]_2[M_2(CO)_8(SR)_2]$ (M = Mo, W; R = Ph, *t*-Bu, Bz) (**1**), are prepared by refluxing $M(CO)_6$ with $[Et_4N]SR$ in acetonitrile. On the basis of analytical, spectroscopic, and conductometric data, they are characterized as 2:1 electrolytes with the dinuclear dianions consisting of two metal(0)–$(CO)_4$ fragments bridged by two μ-SR moieties. The complexes are converted to the corresponding M^I_2 dimers, $M_2(CO)_8(SR)_2$ (**2**), by two-electron electrochemical oxidation (in a single step) (eq i) or treatment with a mild chemical oxidant, to the solvolyzed M^I_2 dimers, $M_2(CO)_6(MeCN)_2(SR)_2$ (**3**), by

$$[M_2(CO)_8(SR)_2]^{2-} \rightleftharpoons [M_2(CO)_8(SR)_2] + 2e^- \quad \text{(i)}$$

oxidation in acetonitrile, and to the monomeric M^0 species, $[M(CO)_5(SR)]^-$ (**4**) (for M = Mo, R = Ph, *t*-Bu), by treatment with excess CO. Interconversion of **1**–**4** by means of redox, solvolysis, and carbonylation reactions and the influence of the solvolysis and carbonylation reactions on electrode reactions (eq i) are described. Oxidation of the M^0_2 to the M^I_2 dimers is accompanied by formation of a single metal–metal bond and significant rearrangement within the $M_2(SR)_2$ core. These changes apparently supply the driving force that enables two-electron transfer to occur in a single step. Comparisons with structurally analogous compounds indicate that contractions of ~1.0 Å in the M–M bond distance and of ~25° in the M–S–M bridge angle accompany $M^0_2 \rightarrow M^I_2$ oxidation. Despite these large displacements in nuclear coordinates, electrode reaction i exhibits Nernstian two-electron behavior by cyclic voltammetry at 0.1 V s^{-1}. This kinetically facile behavior suggests that the nuclear rearrangement involved in conversion of $[M_2(CO)_8(SR)_2]^{2-}$ to $M_2(CO)_8(SR)_2$ is concerted in such a way that a low activation energy barrier is presented to electron transfer.

Introduction

The reactions of thiols and thiolates with metal complexes have received increasing attention in the recent literature. In particular, the chemistry of molybdenum with these reagents has come increasingly under study, with virtually all oxidation states (0–VI) of this metal represented. Mo–SR bonding usually is accompanied in the higher oxidation states by coordination of strong π-donor oxo ligands to the metal and in the lower oxidation states by the presence of π-acceptor ligands such as CO. These coligands provide favorable conditions for Mo–SR binding by moderating the effective nuclear charge of the metal. Compounds with an exclusively Mo–SR coordination shell are known but occur in a smaller number of cases. Examples[1–6] of various oxidation levels

[†] Florida Atlantic University.
[‡] Battelle-Kettering Laboratory.
[§] Visiting Scientist at BKL from the Fujian Institute of Research on the Structure of Matter, Fuzhou, Fujian, The People's Republic of China.

(1) Berg, J. M.; Hodgson, K. O.; Cramer, S. P.; Corbin, J. L.; Elsberry, A. E.; Pariyadath, N.; Stiefel, E. I. *J. Am. Chem. Soc.* **1980**, *101*, 2774.
(2) Bradbury, J. R.; Mackay, M. F.; Wedd, A. G. *Aust. J. Chem.* **1978**, *31*, 2423.
(3) Otsuka, S.; Kamata, M.; Hirotsu, K.; Higuchi, T. *J. Am. Chem. Soc.* **1981**, *103*, 3014.
(4) (a) Sellman, D.; Schwartz, J. *J. Organomet. Chem.* **1983**, *241*, 343. (b) Sellman, D.; Zapf, L. *J. Organomet. Chem.* **1985**, *289*, 57.
(5) Kamata, M.; Yashida, T.; Otsuka, S.; Hirotsu, K.; Higuchi, T. *J. Am. Chem. Soc.* **1981**, *103*, 3572.

0020-1669/87/1326-2524$01.50/0

Table I. Analytical and Yield Data for the Complexes $[Et_4N]_2[M_2(CO)_8(SR)_2]$ (**1**), $[M_2(CO)_8(SR)_2]$ (**2**), and $[M_2(CO)_6(MeCN)_2(SR)_2]$ (**3**) (M = Mo, W; R = H, Ph, *t*-Bu, Bz)

compd	% yield	% CO[a]	% C[b]	% H[b]	% N[b]
1 (M = Mo; R = Ph)	83	99	48.20 (48.32)	5.80 (5.59)	3.08 (3.13)
1 (M = W; R = Ph)	82	97	40.50 (40.37)	4.89 (4.67)	2.27 (2.62)
1 (M = Mo; R = *t*-Bu)	51	96	44.75 (44.96)	7.04 (6.79)	3.06 (3.28)
1 (M = W; R = *t*-Bu)	63		36.88 (37.28)	5.80 (5.63)	2.99 (2.72)
1 (M = Mo; R = Bz)[c]	74	102	48.56 (49.44)	5.76 (5.85)	2.89 (3.03)
1 (M = W; R = Bz)[d]	52		41.36 (41.53)	5.10 (4.91)	2.45 (2.55)
1 (M = Mo; R = H)	36	97	38.56 (38.81)	5.79 (5.66)	4.00 (3.77)
1 (M = W; R = H)	78	96	30.86 (31.37)	4.74 (4.57)	3.04 (3.05)
2 (M = Mo; R = Ph)	86	99	37.74 (37.85)	1.64 (1.57)	
2 (M = W; R = Ph)	88		29.35 (29.63)	1.49 (1.23)	
2 (M = Mo; R = *t*-Bu)	73	96	31.85 (32.32)	3.03 (3.10)	
2 (M = W; R = *t*-Bu)	87		24.51 (24.94)	2.39 (2.33)	
2 (M = Mo; R = Bz)	90	93	39.41 (39.87)	2.25 (2.11)	
2 (M = W; R = Bz)	53		31.62 (31.50)	1.63 (1.67)	
3 (M = Mo; R = Ph)	49		39.51 (40.00)	2.30 (2.42)	4.25 (4.24)
3 (M = W; R = Ph)	25		30.86 (31.58)	1.77 (1.91)	2.93 (3.35)
3 (M = Mo; R = *t*-Bu)	43	101	34.82 (34.84)	4.01 (3.87)	4.29 (4.52)
3 (M = W; R = *t*-Bu)	25		26.34 (27.14)	2.89 (3.02)	2.69 (3.52)
3 (M = Mo; R = Bz)	31		41.75 (41.86)	2.93 (2.91)	3.84 (4.07)
3 (M = W; R = Bz)	39		32.21 (33.33)	2.31 (2.31)	3.02 (3.24)

[a] Percent of predicted value after Br_2 oxidation. [b] Found values with calculated values in parentheses. [c] Mo: 20.22 (20.8). [d] W: 34.23 (33.5).

of molybdenum bound to thiolate include $MoO_2[CH_3SCH_2CH_2N(CH_2CH_2S)_2]$, $[MoO(SPh)_4]^-$, $Mo(S\text{-}t\text{-}Bu)_4$, $Mo(CO)_3(SC_6H_4SCH_3)_2$, $Mo_2(CO)_8(S\text{-}t\text{-}Bu)_2$, and $[Mo(CO)_5(SH)]^-$. Much of the current interest in the chemistry of these compounds arises from the known presence of Mo–S bonding in a variety of molybdoenzymes, among them nitrogenase. Our efforts to model the molybdenum site of this enzyme led us to initiate synthetic studies of low-valent-molybdenum complexes, which might be used as reactants in the preparation of Fe–Mo–S species, the moiety postulated to be present in nitrogenase.[7] In this regard, we have reported preliminary data on the synthesis, characterization, and reactivity of the dinuclear species $[Et_4N]_2[M_2(CO)_8(SR)_2]$ for both molybdenum[8] and tungsten.[9] Of particular interest was the fact that these complexes undergo chemically reversible two-electron oxidation *in a single step*, yielding dinuclear M^I species $[M_2(CO)_8(SR)_2]$. The oxidized complexes exhibited a tendency to undergo solvolysis to $[M_2(CO)_6(solvent)_2(SR)_2]$ species. Herein we provide systematic synthetic procedures for these three series of molybdenum and tungsten complexes, summarize their spectral characterization and chemical reactivity, and describe in detail their two-electron electrochemical behavior.

Experimental Section

Materials and Methods. All synthetic procedures were carried out under an inert atmosphere by using standard Schlenk tube techniques and degassed solvents. MeCN was distilled from CaH_2 and THF from sodium benzophenone ketyl. Toluene, 1,2-dichloroethane, and hexane were dried over molecular sieves prior to use. All other solvents (diethyl ether, Mallinkrodt; DMF, Burdick and Jackson; 2-propanol, Mallinkrodt; methanol, J. T. Baker) were used as received. $Mo(CO)_6$ and $W(CO)_6$ were purchased from Pressure Chemical Co., anhydrous $[Et_4N]Cl$ from Kodak, and CO from Matheson Gas. Sodium thiolate salts were prepared by reaction of stoichiometric amounts of thiol and NaOMe in MeOH, followed by evaporation to dryness, trituration of the residue with diethyl ether, and filtration.

Infrared spectra were recorded on a Beckman IR-20A spectrophotometer and UV/vis spectra on a Cary 118C instrument. Conductivity measurements were made with a Radiometer instrument and calibrated electrode. Elemental analyses for carbon, hydrogen, and nitrogen were determined in-house on a Perkin-Elmer 240 instrument equipped with a Microjector from Control Equipment Corp.

CO evolution experiments were carried out by completely degassing a solution of excess Br_2 in CH_2Cl_2 by using several freeze–pump–thaw cycles and then adding the accurately weighed solid complex to the final frozen solution. After warming to room temperature, the reaction was allowed to proceed for 2 h at which time the mixture was frozen at 77 K and the noncondensable gas transferred via Toepler pumping to a calibrated manometric system where it was quantitated. An aliquot of the gas was then analyzed mass spectrometrically to confirm that it was pure CO.

Elemental analytical, CO evolution, and yield data for all complexes are found in Table I.

Syntheses of Complexes. (a) $[Et_4N]_2[M_2(CO)_8(SR)_2]$ (M = Mo; R = H, Ph, *t*-Bu, Bz. M = W; R = Ph, *t*-Bu) (1). A solution of $[Et_4N][SR]$ was generated by reaction of NaSR (10.0 mmol) with anhydrous $[Et_4N]Cl$ (10.0 mmol) in MeCN (90 mL) at 50 °C for 1.5 h. This slurry was filtered (to remove NaCl) onto solid $M(CO)_6$ (10.0 mmol), and the resulting reaction mixture was stirred at 50 °C for 4 h (M = Mo) or under reflux for 5 h (M = W). After cooling and filtration, the resulting yellow solution was evaporated under vacuum to 30 mL and 100 mL of *i*-PrOH slowly added. The microcrystalline yellow product was isolated by filtration, washed with *i*-PrOH, and dried *in vacuo*.

(b) $[Et_4N]_2[W_2(CO)_8(SBz)_2]$. This complex was prepared as described above except that the reaction was carried out at 45 °C for 18 h.

(c) $[Et_4N]_2[W_2(CO)_8(SH)_2]$. NaSH (10.0 mmol) and anhydrous $[Et_4N]Cl$ (10.0 mmol) were dissolved in EtOH (50 mL), and the solution was stirred at room temperature for 1 h and then filtered. The filtrate was evaporated to dryness under vacuum and solid $W(CO)_6$ (10 mmol) added to the residue followed by THF (100 mL). The reaction mixture was heated under reflux for 1 h, yielding a yellow solid, which was isolated by filtration and washed with THF. The pure product was obtained by recrystallizing this solid from MeCN/*i*-PrOH.

(d) $[M_2(CO)_8(SR)_2]$ (M = Mo, W; R = Ph, *t*-Bu, Bz) (2). $[Et_4N]_2[M_2(CO)_8(SR)_2]$ (0.5 mmol) and I_2 (0.50 mmol) were slurried in toluene under an atmosphere of CO. After 3 h, the slurry was filtered to remove $[Et_4N]I$ and the green filtrate evaporated to dryness under vacuum to yield the product as a dark green solid.

(e) $[M_2(CO)_6(MeCN)_2(SR)_2]$ (M = Mo, W; R = Ph, *t*-Bu, Bz) (3). Method A. $[M_2(CO)_8(SR)_2]$ (0.3 mmol) was added to MeCN (30 mL) and the mixture stirred for 1 h (M = Mo) or 18 h (M = W). The green slurry was filtered to yield the product, which was washed with a small amount of MeCN and dried *in vacuo*. The yield could be increased by evaporation of the reaction mixture and addition of *i*-PrOH, but in some cases a slight loss in analytical purity resulted.

Method B. MeCN (20 mL) was added to a mixture of $[Et_4N]_2[M_2(CO)_8(SR)_2]$ (0.5 mmol) and I_2 (0.5 mmol). After the mixture was stirred at room temperature (4 h for Mo; 18 h for W), the green solid product that had precipitated was isolated by filtration, washed with MeCN, and dried *in vacuo*. The compound $[Ph_3C][BF_4]$ was also effective as an oxidant in MeCN, but its use generally resulted in lower yields.

Interconversion Reactions. Reactions are not demonstrated for all variations of M and R. Typical examples are presented.

(a) $[M^I_2(CO)_6(MeCN)_2(SR)_2]/[M^I_2(CO)_8(SR)_2]$. $[Mo_2(CO)_6(MeCN)_2(S\text{-}t\text{-}Bu)_2]$ (0.25 mmol) was dissolved in CO-saturated toluene

(6) (a) Darensbourg, D. J.; Rokicki, A.; Kudaroski, R. *Organometallics* **1982**, *1*, 1161. (b) Gingerich, R. G. W.; Angelici, R. J. *J. Am. Chem. Soc.* **1979**, *101*, 5604.
(7) Averill, B. A. *Struct. Bonding (Berlin)* **1983**, *53*, 59. Holm, R. H. *Chem. Soc. Rev.* **1981**, *10*, 455.
(8) Zhuang, B.; McDonald, J. W.; Schultz, F. A.; Newton, W. E. *Organometallics* **1984**, *3*, 943.
(9) Zhuang, B.; McDonald, J. W.; Schultz, F. A.; Newton, W. E. *Inorg. Chim. Acta* **1985**, *99*, L29.

(10 mL) and the mixture stirred under a CO atmosphere for 0.5 h. Evaporation to dryness under vacuum gave a green product (0.19 mmol, 75%) whose IR and electronic spectra were identical with those of $[Mo_2(CO)_8(S\text{-}t\text{-}Bu)_2]$ prepared either by our method described above or by that of Otsuka and co-workers.[5] The conversion of $[M_2(CO)_8(SR)_2]$ to $[M_2(CO)_6(MeCN)_2(SR)_2]$ is described above as method A for **3**.

(b) $[M^I_2(CO)_8(SR)_2]/[M^0_2(CO)_8(SR)_2]^{2-}$. MeCN (15 mL) was added to a mixture of $[Mo_2(CO)_8(SPh)_2]$ (0.24 mmol) and $[Et_4N][BH_4]$ (1.0 mmol), and the solution (initially containing both the starting dimer and its MeCN substitution product) was stirred at room temperature for 2 h, during which time the color changed from green to yellow. The reaction mixture was filtered and the filtrate reduced in volume to 8 mL. Addition of *i*-PrOH (20 mL) gave a yellow crystalline product, which was identified as $[Et_4N]_2[Mo_2(CO)_8(SPh)_2]$ by its IR spectrum, in 43% yield. Conversions of $[M_2(CO)_8(SR)_2]^{2-}$ to $[M_2(CO)_8(SR)_2]$ and to $[M_2(CO)_6(MeCN)_2(SR)_2]$ are described above as synthetic procedures for **2** and **3** (method B), respectively.

(c) $[M^0_2(CO)_8(SR)_2]^{2-}/[M^0(CO)_5(SR)]^-$. CO was bubbled through a 1 mM solution of $[Mo_2(CO)_8(SPh)_2]^{2-}$ in MeCN that also contained 0.1 M $[Et_4N][BF_4]$ as supporting electrolyte. The flow was stopped periodically and a cyclic voltammogram recorded. Over a 30-min period the characteristic reversible wave of the starting material at −0.79 V was replaced by an irreversible wave at −0.13 V, which was ascribed to oxidation of $[Mo(CO)_5(SPh)]^-$. Purging the latter solution with argon resulted in the return of the original cyclic voltammogram of $[Mo_2(CO)_8(SPh)_2]^{2-}$.

Electrochemical Measurements. Cyclic voltammetry (CV) and normal-pulse voltammetry (NPV) experiments were carried out with an IBM Instruments Model EC225 voltammetric analyzer. The working electrode was a glassy-carbon disk (area 0.0707 cm^2) from Bioanalytical Systems (BAS). This electrode was polished with 0.05-μm alumina (Buehler) before each use. The Ag/Ag^+ reference electrode consisted of an Ag wire in a 0.01 M $AgNO_3$ plus 0.1 M Bu_4NBF_4 solution in acetonitrile and was separated from the sample solution by a salt bridge containing 0.1 M Bu_4NBF_4 in the solvent of interest. NPV experiments were performed at a potential sweep rate of 4 mV/s and a pulse repetition time of 2 s. During CV experiments, *iR* compensation was achieved by use of positive feedback.

Controlled-potential coulometry (CPC) experiments were performed with an EG&G Princeton Applied Research (PAR) Model 173/179 potentiostat and digital coulometer and a Model 377 coulometry cell. The working electrode was a 45 pores/in. disk of reticulated vitreous carbon (RVC; Energy Research and Generation, Inc., Oakland, CA). The RVC disk measured 36 mm in diameter by 5 mm thick; the calculated surface area was 140 cm^2. A Pt wire introduced through the cell top impaled the RVC disk to achieve electrical contact. The Ag/Ag^+ reference electrode described above was used for these coulometry experiments. The number of transferred electrons was calculated from the charge that had accumulated when the current fell below 1% of its initial value.

DMF and MeCN from Burdick and Jackson were distilled-in-glass reagents and were used as received. The supporting electrolyte, Bu_4NBF_4 from Southwestern Analytical Chemicals, was of electrometric grade. Solutions were deoxygenated and blanketed with argon. All potentials are reported vs. the $E^{\circ\prime}$ of ferrocene, which was added to the sample solution as an internal reference at the end of each experiment. The $E^{\circ\prime}$ of the ferrocene/ferrocenium (Fc/Fc^+) couple was found by cyclic voltammetry to be +0.075 ± 0.018 and +0.087 ± 0.009 V vs. the Ag/Ag^+ reference in DMF and MeCN, respectively.

Results and Discussion

Syntheses. $[Et_4N]_2[M_2(CO)_8(SR)_2]$ (1). Complexes **1** (M = Mo; R = H, Ph, *t*-Bu, Bz. M = W; R = Ph, *t*-Bu, Bz) were prepared by reacting the desired metal hexacarbonyl with 1 equiv of tetraethylammonium thiolate (generated in situ from NaSR and anhydrous $[Et_4N]Cl$) in acetonitrile (eq 1). For the molybdenum system, a reaction time of about 4 h at 45 °C was sufficient for complete conversion of $Mo(CO)_6$ to product for all four thiolate species. If the reaction mixture was heated above this temperature, significant decomposition occurred, as evidenced by formation of a dark brown solution and by decreased yields. Consistent with generally greater inertness of tungsten over molybdenum, formation of the $[W_2(CO)_8(SR)_2]^{2-}$ ion required either higher reaction temperature or longer reaction times. Syntheses of the M = W species for R = *t*-Bu and Ph were readily accomplished in refluxing MeCN (ca. 80 °C) for 5 h, but use of these conditions for R = Bz or H resulted in very dark reaction mixtures that yielded impure products, as evidenced by their IR spectra. For the benzyl system, longer reaction times (ca. 18 h) at a lower temperature (ca. 45 °C) produced the desired compound, albeit in lower yield. We were unable under any set of temperature/reaction time conditions to produce $[W_2(CO)_8(SH)_2]^{2-}$ using MeCN as solvent. However, this complex was synthesized in refluxing THF from stoichiometric amounts of starting materials. As pointed out previously,[9] this result is unexpected, since reaction of [PPN][SH] with $W(CO)_6$ has been shown[6,10,11] to yield $[W(CO)_5(SH)]^-$. It would seem that the solubility difference between the $[Et_4N]^+$ and $[PPN]^+$ salts (the former is insoluble in THF while the latter must be precipitated with Et_2O/hexane) offers a possible explanation for this paradox.

$$2M(CO)_6 + 2[Et_4N][SR] \xrightarrow{MeCN} [Et_4N]_2[M_2(CO)_8(SR)_2] + 4CO \quad (1)$$

The dinuclear dianions (**1**) have been characterized by elemental analyses (Table I) and by IR and UV/vis spectral studies (vide infra). The data are consistent with the proposed formulation. The complexes also release the expected amount of CO (Table I) on oxidation with excess Br_2, conditions that have been shown to degrade low-valent-molybdenum[12] and -tungsten[13] carbonyls with complete loss of carbon monoxide. In addition, we carried out a study of the concentration dependence of the equivalent conductivities of several of these compounds to ascertain if a five-coordinate, mononuclear formulation $[M(CO)_4(SR)]^-$ was possible for these species. Plots of equivalent conductivity vs. the square root of concentration were linear with slopes of ca. −600 units, consistent with the presence of 2:1 electrolytes[14,15] and confirming the postulated formulation of the complexes as dinuclear dianions. This result is of relevance with regard to the presumed monomeric complex, $[Me_4N][Mo(CO)_4(SC_6H_4SCH_3)]$ ($CH_3S\text{-}C_6H_5S^-$ = *o*-(methylthio)benzenethiolate), reported by Sellmann.[4] $[Me_4N][Mo(CO)_4(SC_6H_4SCH_3)]$ has color and infrared spectral properties nearly identical with those of our **1** and is prepared by a similar synthetic procedure. We believe this complex could be formulated as $[Me_4N]_2[Mo_2(CO)_8(SC_6H_4SCH_3)_2]$.

The mechanism of the reaction whereby $[M_2(CO)_8(SR)_2]^{2-}$ is formed is unknown. However, it is pertinent to note that, as pointed out by Gingerich and Angelici[6b] for the synthesis of $[W(CO)_5(SH)]^-$, the reaction rate for our systems is seemingly too rapid to involve simple rate-determining dissociation of CO. One possible mechanism could invoke a nucleophilic attack by thiolate on a carbonyl carbon, a possibility previously explored by Darensbourg and co-workers.[6a] Alternatively, the initial step in reaction 1 may be the formation of an acetonitrile (or THF) derivative of the metal carbonyl. Replacement of CO by MeCN in $Mo(CO)_6$ and $W(CO)_6$ has been demonstrated under both thermal[16] and photolytic[17] reaction conditions. In any case, it seems remarkable that $[M_2(CO)_8(SR)_2]^{2-}$ complexes have not been previously prepared or recognized, given the past and recent interest in metal–carbonyl–thiolate species.[4-6,18-22]

(10) Angelici, R. J.; Gingerich, R. G. W. *Organometallics* **1983**, *2*, 89.
(11) Heberhold, M.; Suss, G. *J. Chem. Res., Miniprint*, **1979**, 2720.
(12) McDonald, J. W.; Corbin, J. L.; Newton, W. E. *J. Am. Chem. Soc.* **1975**, *97*, 1970.
(13) Templeton, J. L.; Herrick, R. S.; Rusik, C. A.; McKenna, C. E.; McDonald, J. W.; Newton, W. E. *Inorg. Chem.* **1985**, *24*, 1383.
(14) Davison, A.; Howe, D. V.; Shawl, E. T. *Inorg. Chem.* **1967**, *6*, 458.
(15) Callahan, K. P.; Cichon, E. J. *Inorg. Chem.* **1981**, *20*, 1941.
(16) Tate, D. P.; Knipple, W. R.; Augl, J. M. *Inorg. Chem.* **1962**, *1*, 433.
(17) Dobson, G. R.; Amer El Sayed, M. F.; Stolz, I. W.; Sheline, R. K. *Inorg. Chem.* **1962**, *1*, 527.
(18) Benson, I. B.; Killops, S. D.; Knox, S. A. R.; Welch, A. J. *J. Chem. Soc., Chem. Commun.* **1980**, 1137.
(19) (a) Kaul, B. B.; Sellman, D. *Z. Naturforsch., B: Anorg. Chem., Org. Chem.* **1983**, *38B*, 562. (b) Sellman, D.; Ludwig, W. *J. Organomet. Chem.* **1984**, *269*, 171.
(20) (a) Dilworth, J. R.; Hutchinson, J.; Zubieta, J. A. *J. Chem. Soc., Chem. Commun.* **1983**, 1034. (b) Blower, P. J.; Dilworth, J. R.; Hutchinson, J.; Nicholson, T.; Zubieta, J. A. *J. Chem. Soc., Dalton Trans.* **1985**, 2639.
(21) (a) Schulze, W.; Ziegler, M. L. *Z. Anorg. Allg. Chem.* **1981**, *481*, 78. (b) Hohmann, M.; Krauth-Siegel, L.; Wiedenhammer, K.; Schulze, W.; Ziegler, M. L. *Z. Anorg. Allg. Chem.* **1981**, *481*, 95.

Table II. Infrared and UV/Vis Spectral Data for the Complexes $[Et_4N]_2[M_2(CO)_8(SR)_2]$ (**1**), $[M_2(CO)_8(SR)_2]$ (**2**), and $[M_2(CO)_6(MeCN)_2(SR)_2]$ (**3**)

compd	IR[a]	UV/vis[b]
1 (M = Mo; R = Ph)	2000 m, 1920 s, 1860 s, 1790 s	375 (2720)[c]
1 (M = W; R = Ph)	2000 m, 1910 s, 1885 s, 1790 s	450 sh, 410 sh, 388 (2100)[c]
1 (M = Mo; R = *t*-Bu)	2000 m, 1900 s, 1850 s, 1790 s	385 (2180)[c]
1 (M = W; R = *t*-Bu)	2000 m, 1890 s, 1845 s, 1795 s	388 (1990)[c]
1 (M = Mo; R = Bz)	2000 m, 1905 s, 1845 s, 1780 s	425 sh, 400 (2350)[c]
1 (M = W; R = Bz)	2000 m, 1900 s, 1840 s, 1770 s	420 sh, 400 (1890)[c]
1 (M = Mo; R = H)	2000 m, 1900 s, 1845 s, 1780 s	415 sh, 375 (2680)[c]
1 (M = W; R = H)	2000 m, 1900 s, 1840 s, 1780 s	425 sh, 390 (2480)[c]
2 (M = Mo; R = Ph)	2020 m, 2000 s, 1980 s	640 (660), 422 (10 100), 345 (9130)[d]
2 (M = W; R = Ph)	2020 m, 1980 s, 1965 s	612 (1130), 415 (10 400), 340 sh[d]
2 (M = Mo; R = *t*-Bu)	2015 m, 2000 s, 1970 s	650 (650), 405 (14 100)[d]
2 (M = W; R = *t*-Bu)	2020 m, 2010 m, 1980 s, 1950 s	622 (1910), 400 (13 100)[d]
2 (M = Mo; R = Bz)	2020 m, 1980 s, 1970 s	620 (610), 405 (13 900)
2 (M = W; R = Bz)	2020 m, 1970 s	592 (1090), 398 (15 300)[d]
3 (M = Mo; R = Ph)	2040 w, 1990 s, 1950 s, 1900 s	700 (760), 432 (10 700), 335 (18 900)[c]
3 (M = W; R = Ph)	2040 w, 1980 s, 1935 s, 1855 s	680 (760), 426 (8000), 320 (14 000)[c]
3 (M = Mo; R = *t*-Bu)	2030 w, 2000 s, 1950 s, 1870 s	720 (880), 420 (12 000), 340 (13 100)[c]
3 (M = W; R = *t*-Bu)	2030 w, 1985 s, 1935 s, 1880 s	690 (960), 412 (9220), 339 (12 000)[c]
3 (M = Mo; R = Bz)	2040 w, 1985 s, 1955 s, 1850 s	675 (520), 420 (9200), 350 (13 200)[c]
3 (M = W; R = Bz)	2050 w, 1980 s, 1955 s, 1860 s	665 (860), 418 (8300), 344 (15 400)[c]

[a] Values of CO stretching in cm^{-1}. Spectra taken as KBr pellets. [b] Values in nm with molar absorptivities in parentheses. [c] MeCN solution. [d] Hexane solution.

$[M_2(CO)_8(SR)_2]$ (2). The molybdenum complex of this form for R = *t*-Bu was prepared by Otsuka and co-workers,[3,5] from reaction of $Mo(SR)_4$ with CO in toluene. However, since the metal-containing starting material has not been prepared for tungsten or for other thiolate ligands, the scope of this procedure is limited to this single system. Also, tungsten complexes of type **2** with a variety of thiolate ligands were prepared in relatively low yields by Hüttner and co-workers via photolysis of $W(CO)_6$/thiol or $W(CO)_6$/disulfide mixtures in toluene.[22] We were able to prepare a variety of complexes of this form in good yield for both molybdenum and tungsten by oxidizing the $[M_2(CO)_8(SR)_2]^{2-}$ (M = Mo, W; R = Ph, *t*-Bu, Bz) dianions with a stoichiometric amount of iodine in CO-saturated toluene (eq 2). The use of

$$[Et_4N]_2[M_2(CO)_8(SR)_2] + I_2 \rightarrow [M_2(CO)_8(SR)_2] + 2[Et_4N]I \quad (2)$$

excess CO was implemented as a precaution to prevent decarbonylation of the product. Filtration to remove $[Et_4N]I$ and evaporation of the filtrate yielded the desired species, which, due to their extreme solubility in most solvents, were difficult to obtain in crystalline form. However, products generated in this way were analytically pure and had IR and electronic spectral properties (vide infra) consistent with our proposed formulation and with data previously reported[3,5,22] for complexes of this type.

Attempts to prepare $[M_2(CO)_8(SH)_2]$ using the method outlined in eq 2 met with no success. Addition of I_2 to toluene solutions of **1** (M = Mo, W; R = H) did not produce the immediate green color of $[M_2(CO)_8(SR)_2]$, and only ill-characterized brown solids could be obtained from these mixtures. $[W_2(CO)_8(SH)_2]$ has been prepared[11] by photolysis of $[W(CO)_5SH_2]$, showing that, while this species exists, it apparently cannot be prepared by chemical oxidation of **1**. Electrochemical data for the **1** (R = H) species support this conclusion. We observe irreversible waves for the oxidation of $[Mo_2(CO)_8(SH)_2]^{2-}$ and $[W_2(CO)_8(SH)_2]^{2-}$ at −0.84 and −0.78 V, respectively.

$[M_2(CO)_6(MeCN)_2(SR)_2]$ (3). Initially, we attempted to prepare $[M_2(CO)_8(SR)_2]$ by I_2 oxidation of $[Et_4N]_2[M_2(CO)_8(SR)_2]$ in MeCN. Although a facile reaction occurred in this solvent, elemental analytical results for the products showed the presence of nitrogen, and IR and electronic spectral data for the Mo/S-*t*-Bu system were not consistent with those reported[3,5] for $[Mo_2(CO)_8(S\text{-}t\text{-}Bu)_2]$. This information suggested the presence of coordinated MeCN in the products, and indeed we were able to fit the above data plus CO evolution results to the formulation $[M_2(CO)_6(MeCN)_2(SR)_2]$. These solvent-substituted complexes also can be prepared by stirring $[M_2(CO)_8(SR)_2]$ in MeCN, indicating that the dinuclear hexacarbonyl species are formed in a multistep reaction involving initial oxidation to the M(I) octacarbonyl followed by thermal solvolysis of this complex (eq 3 and 4). Although the monosubstituted MeCN complex $[M_2(CO)_7(MeCN)(SR)_2]$ was not isolated, electrochemical evidence for its existence is described in a subsequent section.

$$[Et_4N]_2[M_2(CO)_8(SR)_2] + I_2 \rightarrow [M_2(CO)_8(SR)_2] + 2[Et_4N]I \quad (3)$$

$$[M_2(CO)_8(SR)_2] + 2MeCN \rightarrow [M_2(CO)_6(MeCN)_2(SR)_2] + 2CO \quad (4)$$

The rates of solvolysis of $[M_2(CO)_8(SR)_2]$ are markedly metal-dependent. Thus, the product isolated 1 h after addition of I_2 to $[M_2(CO)_8(SR)_2]^{2-}$ for M = Mo is exclusively the disolvated species, while for M = W only the unsubstituted complex **2** is present after this time. Reaction times of 18 h and/or heating of the oxidized reaction mixtures are necessary for conversion to $[W_2(CO)_6(MeCN)_2(SR)_2]$. Even under these conditions, the somewhat low nitrogen percentages (Table I) may indicate incomplete attainment of the disolvated species. For both Mo and W, no products indicative of further substitution of CO by MeCN beyond $[M_2(CO)_6(MeCN)_2(SR)_2]$ were isolated even after prolonged reaction times.

Attempts to isolate pure solvated species containing coordinated DMF met with less success. While both I_2 oxidation of $[Mo_2(CO)_8(SR)_2]^{2-}$ in DMF and reaction of $[Mo_2(CO)_8(SR)_2]$ with pure DMF (as in eq 3 and 4 for MeCN) yielded green solids, elemental analytical data were not consistent with formulation of the products as either $[Mo_2(CO)_6(DMF)_2(SR)_2]$ or $[Mo_2(CO)_7(DMF)(SR)_2]$. The UV/vis spectra of the solids were similar to those exhibited by $[Mo_2(CO)_6(MeCN)_2(SR)_2]$, and the IR spectra contained bands at 1600–1700 cm^{-1}, which can reasonably be assigned to coordinated DMF. On the basis of these results, we speculate that $[Mo_2(CO)_8(SR)_2]$ does in fact undergo solvolytic decarbonylation in DMF but that, for reasons yet undetermined, it is more difficult to obtain pure solid products than in MeCN. Electrochemical results (vide infra) support this conclusion. We were unable to obtain even semipure DMF solvates for the tungsten system although our examination of this reactivity pattern was cursory.

Spectra. Infrared and UV/vis spectral data for all compounds of types **1**, **2**, and **3** are summarized in Table II. In addition, spectra of these species for the Mo/S-*t*-Bu system are shown in Figure 1 as an aid to future characterization. The spectral patterns

(22) Winter, A.; Scheidsteger, O.; Hüttner, G. *Z. Naturforsch., B: Anorg. Chem., Org. Chem.* **1983**, *38B*, 1525.

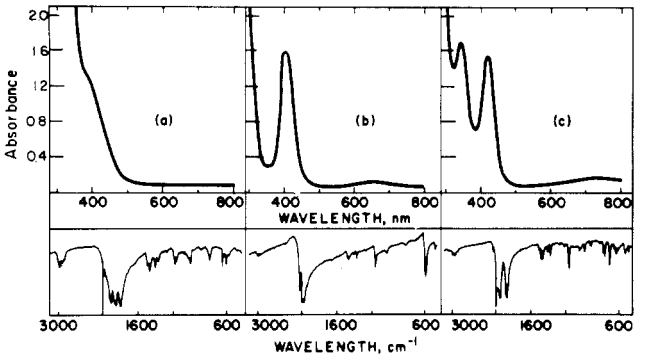

Figure 1. Electronic and infrared spectra of (a) **1**, (b) **2**, and (c) **3** for M = Mo and R = *t*-Bu. Electronic spectra of **1** and **3** were obtained in MeCN; the solvent for **2** was hexane. Infrared spectra were recorded on KBr pellets.

exhibited there are typical of both Mo and W complexes for all thiolate ligands.

The CO stretching region in the infrared spectra of **1** is characterized by a four-band pattern between 1750 and 2000 cm^{-1},

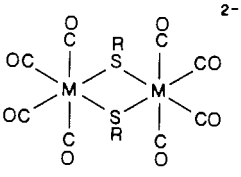

1

consistent with the binuclear formulation of two $M(CO)_4$ fragments bridged by two μ-SR moieties. The electronic spectra of these yellow complexes are relatively featureless and contain only a band at ca. 400 nm with no marked dependence of position or intensity on the nature of the metal or thiolate ligand.

The infrared spectra of the type **2** complexes are consistent with those reported previously[3,5,22] for the structurally characterized species $[Mo_2(CO)_8(S\text{-}t\text{-}Bu)_2]$ and $[W_2(CO)_8(SMe)_2]$ and contain

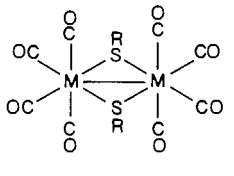

2

a medium-intensity band at ca. 2020 cm^{-1} and a pattern of typically two strong peaks in the 1970–2000-cm^{-1} region. These bright green compounds exhibit electronic spectra containing a relatively weak band at 600–650 nm and a much more intense peak at 400–425 nm. The energies of these bands are dependent on the nature of M and R (Table II). In order for the metals in these neutral dinuclear species to comply with the 18-electron rule, the presence of a single metal–metal bond is required and indeed observed[3,5,22] in the structures of $[Mo_2(CO)_8(S\text{-}t\text{-}Bu)_2]$ and $[W_2(CO)_8(SMe)_2]$. A single metal–metal bond also is predicted from electronic structural analysis[23] of such edge-sharing bioctahedral complexes. The d^5–d^5 $[M_2(CO)_8(SR)_2]$ complexes are predicted to have the configuration $\pi^2\delta^{*2}\delta^2\sigma^2\pi^{*2}$. Thus, the bands at 600–650 and 400–425 nm, which are absent in the non-M–M-bonded complexes ($\pi^2\delta^{*2}\delta^2\sigma^2\pi^{*2}\sigma^{*2}$ configuration), are assigned to $d\pi^* \rightarrow d\sigma^*$ and $d\sigma \rightarrow d\sigma^*$ transitions, respectively.

Scheme I

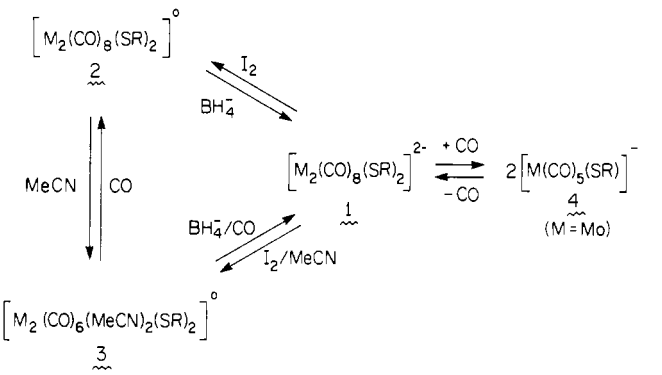

The type **3** complexes exhibit IR spectra containing three strong C≡O stretching frequencies between 1870 and 2000 cm^{-1} and a weak band at higher energy. The lack of complexity in these

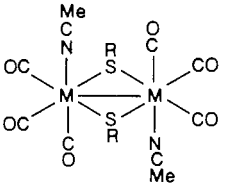

3

CO stretching patterns suggests a symmetric distribution of ligands with one MeCN on each metal. Indeed, a recent structural determination of $[Mo_2(CO)_6(MeCN)_2(SCH_2COOEt)_2]$ by Zhuang and co-workers[26b] demonstrates that the coordinated MeCN moieties in this complex assume a trans-axial geometry as shown in structure **3**. No bands are observed in the 2100–2400-cm^{-1} region that can be assigned to the C≡N stretch of coordinated MeCN. The electronic structures of the type **2** and **3** complexes should be similar, and the low-energy bands in the electronic spectra of the latter are assigned to similar transitions.

Interconversion Reactions. As we noted previously[8,9] and described in the Experimental Section, complex types **1**, **2**, and **3** can be interconverted by means of chemical redox, solvolysis, and carbonylation reactions. This chemistry is summarized in Scheme I. Thus, **1** is converted to **2** by oxidation with a stoichiometric amount of I_2 in toluene and to **3** when this reaction is carried out in MeCN. These reactions can be reversed by reducing **2** or **3** with $[Et_4N]BH_4$ in MeCN. In addition, **2** is converted to **3** by simple treatment with MeCN, whereas exposing a solution of **3** to CO yields **2**. Finally, treating a solution of **1** (M = Mo, R = Ph, *t*-Bu; reaction for R = Bz was not examined) with CO yields species detected by electrochemical measurements (vide infra), which we assign to the mononuclear complex $[Mo(CO)_5(SR)]^-$ (**4**). The reactions are reversed by purging with an inert gas, a fact that has contributed to our inability to isolate solid products. We base our identification on the fact that the analogous $[M(CO)_5(SH)]^-$ species are well characterized,[6,10] although we are unaware of any alkane- or arenethiolates with this stoichiometry. Conversion of **1** to **4** is 100% complete for M = Mo, R = Ph and about 40% complete (1-h treatment) for M = Mo, R = *t*-Bu. The $[W_2(CO)_8(SR)_2]^{2-}$ complexes fail to show significant reactivity with carbon monoxide. Interconversion reactions were not attempted for the SH^--bridged complexes.

Electrochemistry. The electrochemical behavior of the type **1** complexes was investigated by cyclic voltammetry, normal-pulse voltammetry, and controlled-potential coulometry in dimethylformamide and acetonitrile. These compounds undergo reversible two-electron oxidation in a single step in these solvents. This result is illustrated by the cyclic voltammogram in Figure 2 for oxidation of $[W_2(CO)_8(SPh)_2]^{2-}$ plus added ferrocene in DMF. The peak

(23) (a) Shaik, S.; Hoffman, R.; Fisel, C. R.; Summerville, R. H. *J. Am. Chem. Soc.* **1980**, *102*, 4555. (b) Cotton, F. A.; Diebold, M. P.; O'Connor, C. J.; Powell, G. L. *J. Am. Chem. Soc.* **1985**, *107*, 7438. (c) Chakravarty, A. R.; Cotton, F. A.; Diebold, M. P.; Lewis, D. B.; Roth, W. J. *J. Am. Chem. Soc.* **1986**, *108*, 971.

(24) Bradbury, J. R.; Schultz, F. A. *Inorg. Chem.* **1986**, *25*, 4408.

(25) A similar two-stage substitution of $P(n\text{-}Bu)_3$ for CO is observed in the solution dynamics of the analogous phosphido-bridged Mo^I_2 complex, $Mo_2(CO)_8(PEt_2)_2$: Basato, M. *J. Chem. Soc., Dalton Trans.* **1986**, 217.

(26) (a) Zhuang, B.; Huang, L.; Yang, Y.; Lu, J. *Jiego Huaxue* **1985**, *4*, 103. (b) Zhuang, B.; Huang, L.; Yang, Y.; Lu, J. *Inorg. Chim. Acta* **1986**, *116*, L41.

Table III. Electrochemical Data for Oxidation of $[M_2(CO)_8(SR)_2]^{2-}$ Complexes[a]

M	R	CV[b,d] $E^{\circ\prime}$, V	CV[b,d] ΔE_p, V	CV[b,d] $i_p/v^{1/2}AC$	CV[b,d] i_{pc}/i_{pa}	NPV[c,d] $E_{1/2}$, V	NPV[c,d] i_d/AC	CPC n
				Dimethylformamide				
Mo	Ph	−0.771	0.026	1420	0.90	−0.775	1170 (1230)	1.80
W	Ph	−0.772	0.023	1450	1.01	−0.748	1190	1.94
Mo	*t*-Bu	−0.918	0.027	950 (1100)	0.64	−0.968	950 (1240)	1.31
W	*t*-Bu	−0.918	0.034	1200 (1230)	0.96	−0.885	1170 (1280)	1.40
Mo	Bz	−0.947	0.031	1220	0.95	−0.943	1020	1.41
W	Bz	−0.937	0.031	1250	1.00	−0.927	1000	1.60
				Acetonitrile				
Mo	Ph	−0.793	0.025	1980 (2280)	0.94	−0.790	1500 (1960)	
W	Ph	−0.803	0.025	1850 (1970)	0.94	−0.809	1430 (1600)	
Mo	*t*-Bu	−0.964	0.038	1300 (2050)	0.52	−0.951	1310 (1520)	
W	*t*-Bu	−0.945	0.036	1290 (1330)	0.91	−0.937	740 (990)	
Mo	Bz	−0.970	0.035	1450 (1570)	0.87	−0.976	970 (1190)	
W	Bz	−0.961	0.031	2150	0.97	−0.962	1700 (1740)	

[a] Complex concentration ranged from 0.5 to 2.0 mM. Solutions were 0.10 M in $[Bu_4N]BF_4$. All potentials are vs. $E^{\circ\prime}$ of ferrocene. [b] Sweep rate 0.10 V/s. At glassy carbon. [c] Pulse interval 2 s; sweep rate 4 mV/s. At glassy carbon. [d] Values in parentheses are the sum of current parameters for all oxidation waves. Calculated as described in the text.

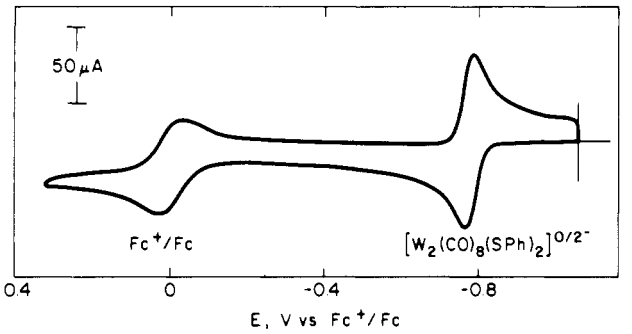

Figure 2. Cyclic voltammogram of 1.79 mM $[W_2(CO)_8(SPh)_2]^{2-}$ with added ferrocene in DMF. Sweep rate: 0.10 V/s.

potential separations in this figure are 59 mV for ferrocene oxidation and 24 mV for $[W_2(CO)_8(SPh)_2]^{2-}$ oxidation, close to the $57/n$ mV values expected for Nernstian transfer of one and two electrons, respectively. The NPV current parameter for $[W_2(CO)_8(SPh)_2]^{2-}$ oxidation in DMF is 1190 μA cm^{-2} mM^{-1}. This is twice the value determined (i.e., 590 μA cm^{-2} mM^{-1})[24] for a one-electron transfer in this solvent. Controlled-potential coulometric oxidation of $[W_2(CO)_8(SPh)_2]^{2-}$ at −0.4 V requires 1.94 faradays/mol of dimer. Thus, electrochemical oxidation of $[W_2(CO)_8(SPh)_2]^{2-}$ is confirmed to be a two-electron process. A similar charge transfer is observed for all type **1** complexes and is represented by the electrode

$$[M_2(CO)_8(SR)_2]^{2-} \rightleftharpoons [M_2(CO)_8(SR)_2]^0 + 2e^- \quad (5)$$

reaction. Electrochemical data for this reaction are presented in Table III. The formal potentials exhibit some dependence on the nature of the thiol substituent but virtually none on the identity of M.

Despite the simplicity of eq 5, both the $[M_2(CO)_8(SR)_2]^{2-}$ and $M_2(CO)_8(SR)_2$ complexes enter into chemical transformations that make the observed electrochemical behavior more complicated. The cyclic voltammogram in Figure 3a for oxidation of $[Mo_2(CO)_8(SPh)_2]^{2-}$ in MeCN displays, in addition to a reversible couple at −0.793 V corresponding to eq 5, other features that are exhibited, to a greater or lesser extent, by most members of this series. The small anodic wave at −0.93 V is attributed to oxidation of $[Mo_2(CO)_7(MeCN)(SPh)_2]^{2-}$ formed by solvolysis of the starting complex.

$$[Mo_2(CO)_8(SR)_2]^{2-} + MeCN \rightleftharpoons [Mo_2(CO)_7(MeCN)(SR)_2]^{2-} + CO \quad (6)$$

This additional wave is observed only for the M = Mo, R = Ph, Bz complexes in MeCN and, consistent with its postulated origin, is eliminated by briefly purging the solution with CO. Accordingly, solvolysis in the M^0_2 oxidation level is slight compared with that

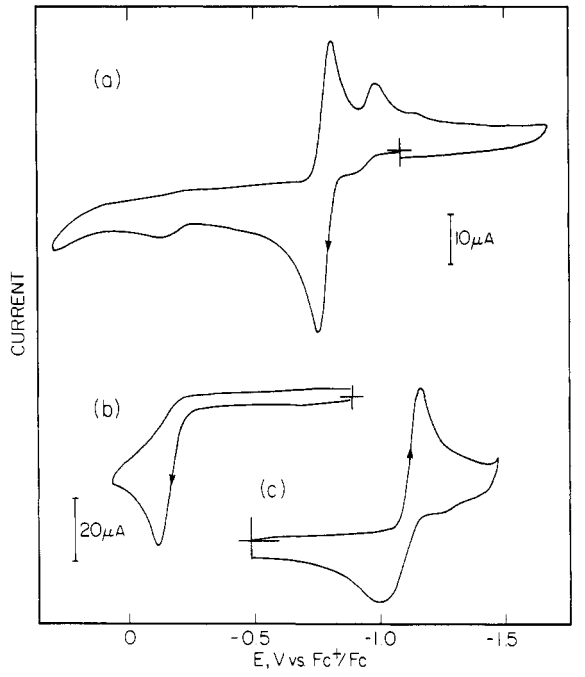

Figure 3. Cyclic voltammograms in MeCN: (a) 1 mM $[Mo_2(CO)_8(SPh)_2]^{2-}$; (b) 1.2 mM solution of this complex after purging with CO for 60 min; (c) 1 mM $[Mo_2(CO)_6(MeCN)_2(SPh)_2]$. Sweep rate: 0.1 V s^{-1} (a, c); 0.05 V s^{-1} (b).

of M^I_2 species (vide infra). In addition, an irreversible anodic wave is observed at −0.13 V upon extension of the positive voltammetric sweep. This wave is assigned to oxidation of the monomeric complex $[Mo(CO)_5(SPh)]^-$ formed by reaction of **1** with solvolytically released CO as described in the previous section.

$$[Mo_2(CO)_8(SPh)_2]^{2-} + 2CO \rightleftharpoons 2[Mo(CO)_5(SPh)]^- \quad (7)$$

The $[Mo(CO)_5(SPh)]^-$ oxidation wave is enhanced at the expense of the $[Mo_2(CO)_8(SPh)_2]^{2-}$ and $[Mo_2(CO)_7(MeCN)(SPh)_2]^{2-}$ oxidation waves if a solution of the octacarbonyl dimer is intentionally reacted with CO. After the solution is purged with CO for 60 min, only the −0.13 V oxidation wave remains (Figure 3b). If this solution is then purged with N_2 or Ar, the original voltammetric trace is restored (Figure 3a), indicating that interconversion of species **1** and **4** is reversible.

Figure 3a also shows that if the CV sweep is reversed following the primary oxidation wave of $[Mo_2(CO)_8(SPh)_2]^{2-}$, three cathodic peaks are observed. These three reduction waves also are observed in MeCN solutions of the corresponding type **2** and **3** complexes in the presence of CO.[8] The cathodic peak potential of the most negative wave is the same as that observed for a solution of

Table IV. Cyclic Voltammetric Peak Potentials[a] for Reduction of $[M_2(CO)_8(SR)_2]$, $[M_2(CO)_7(solv)(SR)_2]$, and $[M_2(CO)_6(solv)_2(SR)_2]$

M	R	E_{pc}, V $[M_2(CO)_8(SR)_2]$	$[M_2(CO)_7(solv)(SR)_2]$	$[M_2(CO)_6(solv)_2(SR)_2]$
		Dimethylformamide		
Mo	Ph	−0.78	−1.03	−1.24
W	Ph	−0.78	−1.10	*b*
Mo	*t*-Bu	−0.93	−1.24	−1.48
W	*t*-Bu	−0.93	−1.27	−1.54
Mo	Bz	−0.96	−1.24	*b*
W	Bz	−0.95	−1.28	*b*
		Acetonitrile		
Mo	Ph	−0.80	−0.98	−1.16
W	Ph	−0.82	−1.00	−1.21
Mo	*t*-Bu	−0.98	−1.16	−1.38
W	*t*-Bu	−0.96	−1.15	*b*
Mo	Bz	−0.99	−1.15	−1.41
W	Bz	−0.98	−1.18	*b*

[a] Potentials are vs. $E^{\circ\prime}$ of Fc/Fc^+. Solutions were 0.10 M in Bu_4NBF_4. Sweep rate 0.10 V/s. At glassy carbon. [b] Reduction not observed.

Scheme II

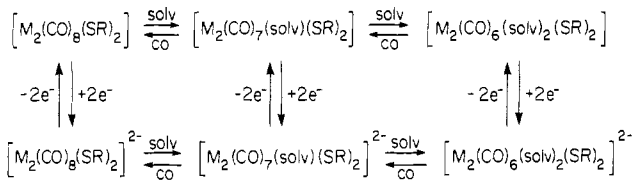

$Mo_2(CO)_6(MeCN)_2(SPh)_2$ (**3**), whose cyclic voltammogram is shown in Figure 3c. The wave at intermediate potential is assigned to $Mo_2(CO)_7(MeCN)(SPh)_2$. These additional cathodic waves arise from solvolysis of the primary Mo^I_2 electrode product.

$$Mo_2(CO)_8(SPh)_2 + MeCN \rightleftharpoons Mo_2(CO)_7(MeCN)(SPh)_2 + CO \quad (8)$$

$$Mo_2(CO)_7(MeCN)(SPh)_2 + MeCN \rightleftharpoons Mo_2(CO)_6(MeCN)_2(SPh)_2 + CO \quad (9)$$

Similar solvolytic behavior is exhibited to varying extents by all $M_2(CO)_8(SR)_2$ complexes in MeCN and DMF. Table IV presents cathodic peak potentials assigned to reduction of the resulting $M_2(CO)_8(SR)_2$, $M_2(CO)_7(solv)(SR)_2$, and $M_2(CO)_6(solv)_2(SR)_2$ (solv = MeCN, DMF) species. These potentials were obtained from cyclic voltammetric experiments involving (a) solutions of **1**, (b) solutions of **1** subjected to coulometric oxidation, and (c) solutions of **3**. In cases where a species was detected by more than one method, the measured peak potential was the same. Table IV shows that each replacement of CO by solvent results in a negative shift in E_{pc} of 200–300 mV, consistent with the relative electron-donor and -acceptor capabilities of these ligands.

An interpretation of the combined electrochemical and solvolytic behavior of the $M_2(CO)_8(SR)_2$ and $[M_2(CO)_8(SR)_2]^{2-}$ complexes is presented in Scheme II. The chemistry described there is understandable in terms of the two-electron redox chemistry found in eq 5 and the relative tendencies of the M(0) and M(I) oxidation states to exchange π-acceptor CO ligands for σ-donor solvent ligands. Starting with $[M_2(CO)_8(SR)_2]^{2-}$, we find that the octacarbonyl form is generally stable with regard to solvolysis in this oxidation state. When solvolysis does occur (e.g., Figure 3a), it is slight and readily reversed by treatment with CO. Here, the solv/CO equilibria are displaced to the left, reflecting the predominance of metal–carbonyl back-bonding in the M(0) oxidation state. In the M(I) oxidation state there is an increased tendency to bind ligands with σ-donor character and the solv/CO equilibria are shifted more extensively to the right. Consequently, solvolysis is initiated by two-electron oxidation of the M(0) dimers and proceeds from left to right along the pathway described in the upper half of Scheme II. In line with our ability to prepare type **3** complexes by a solvolytic route (Scheme I), replacement of CO by solvent can proceed to the hexacarbonyl species. The cyclic voltammetry experiment in Figure 3a provides a dynamic picture of this process and indicates the stepwise nature of the substitution reactions.[25]

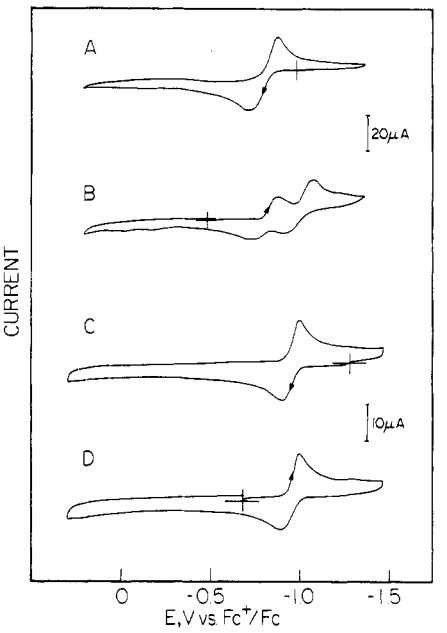

Figure 4. Cyclic voltammograms: (A) 0.75 mM $[W_2(CO)_8(SPh)_2]^{2-}$ in MeCN; (B) prior solution after coulometric oxidation at −0.48 V; (C) 0.50 mM $[W_2(CO)_8(SBz)_2]^{2-}$ in DMF; (D) prior solution after coulometric oxidation at −0.68 V. Sweep rate: 0.1 V s^{-1}.

Table III contains CV peak current ratios (i_{pc}/i_{pa}) which indicate that solvent, metal, and thiol substituent group all influence the rate of the first solvolysis reaction (eq 8) in the M^I_2 oxidation state. Values of $i_{pc}/i_{pa} \sim 1$ are observed for all M = W species. Thus, substitution proceeds more slowly at M = W than at M = Mo centers. Examination of i_{pc}/i_{pa} values for M = Mo reveals that the following trends in reactivity exist with regard to solvent (MeCN > DMF) and thiol substituent group (*t*-Bu > Ph > Bz). Some compounds undergo solvolysis at rates that are too slow to be observed on the time scale of cyclic voltammetry experiments. However, the consequences of these reactions are apparent upon voltammetric examination of $[M_2(CO)_8(SR)_2]^{2-}$ solutions subjected to coulometric oxidation. Panel A in Figure 4 shows that oxidation of $[W_2(CO)_8(SPh)_2]^{2-}$ in MeCN appears as an unperturbed two-electron transfer on the CV time scale. Examination of this solution after coulometric oxidation reveals a mixture of $[W_2(CO)_8(SPh)_2]^{0/2-}$ and $[W_2(CO)_7(MeCN)(SPh)_2]^{0/2-}$ redox couples (panel B). With one exception, all $M_2(CO)_8(SR)_2$ complexes were found to undergo at least one step in the M^I_2 solvolysis sequence depicted in Scheme II. The combination of $[W_2(CO)_8(SBz)_2]^{0/2-}$ in DMF is unique in that the M^0_2 and M^I_2 species can be interconverted on the coulometric time scale without significant change. This result is shown in panels C and D of Figure 4.

The existence of chemical reactions 6–9 requires that additional factors be considered in verifying the two-electron character of electrode reaction 5. The M^0_2 dianions undergo to varying extents solvolysis (eq 6) and carbonylation (eq 7) reactions that lead to lower measured current and charge parameters for $[M_2(CO)_8(SR)_2]^{2-}$ oxidation. Reaction 7 is particularly troublesome because it is driven by CO released from solvolysis of both the M^0_2 starting complex (eq 6) and M^I_2 electrode product (eq 8 and 9) and produces a material oxidizable at a potential more positive than that of the original M^0_2 oxidation wave (Figure 3a). Consequently, controlled-potential coulometry carried out several hundred millivolts positive of eq 5 frequently results in $n < 2$ for oxidation of type **1** complexes. Our approach has been to sum the NPV current parameters for waves assignable to $[M_2(CO)_7(solv)$-

Table V. Structural Data for $[M_2(CO)_8(SR)_2]^0$ and $[M_2(CO)_8(SR)_2]^{2-}$ Complexes

M	R	M-M, Å	M-S, Å	M-S-M, deg	ref
Mo(0)	CH_2CO_2Et	3.939	2.586	99.2	26a
Mo(I)	*t*-Bu	2.984	2.48	73.9	5
W(I)	*t*-Bu	2.988	2.48	74.2	21
W(I)	Me	2.970	2.478	73.8	22

$(SR)_2]^{2-}$, $[M_2(CO)_8(SR)_2]^{2-}$, and $[M(CO)_5(SR)]^-$ oxidation and to compare the results with values expected for two-electron transfer in DMF (1180 μA cm^{-2} mM^{-1}) and MeCN (1940 μA cm^{-2} mM^{-1}).[24] In making these comparisons, we assume that all species have equal diffusion coefficients and transfer the same number of electrons per metal atom in their electrode reactions. Table III shows that the summed values of i_d/AC for M = Mo, W and R = Ph, *t*-Bu in DMF range between 1190 and 1280 μA cm^{-2} mM^{-1}, in excellent agreement with the result expected for two-electron transfer. Coulometric results for the R = Ph species also approximate $n = 2$ in this solvent. The R = Bz compounds in DMF fit the pattern of two-electron behavior; however, their current and charge parameters are ~25% lower than expected. Low compound purity is possible, but these species exhibit satisfactory analytical results and their voltammograms display no additional oxidation waves that can be attributed to decomposition of M(0) dimers. Thus, the factors responsible for these low results cannot be established with certainty from the data at hand.

Electrochemical results in MeCN are influenced by the fact that solvolysis and carbonylation reactions proceed more rapidly in this solvent. Even so, total NPV current parameters for four of the six compounds in MeCN approach the value expected for a two-electron transfer. The remaining low values of i_d/AC are believed to be the result of M^0_2 decomposition, possibly induced by chemical reactivity beyond that described by eq 6–9.

The voltammetric and coulometric results described above indicate that oxidation of complexes **1** involves loss of two electrons at the same potential (eq 5). The two-electron nature of this reaction is attributed to formation of a metal–metal bond in the M^I_2 oxidation state, giving an 18-electron configuration around each metal atom. The M^0_2 complexes satisfy the 18-electron rule without a metal–metal bond. In electronic structural terms[23a] oxidation of these compounds corresponds to a change in configuration from $\pi^2\delta^{*2}\delta^2\sigma^2\pi^{*2}\sigma^{*2}$ to $\pi^2\delta^{*2}\delta^2\sigma^2\pi^{*2}$ with formation of a metal–metal bond at the d^5–d^5 oxidation level. Bond formation would result in structural rearrangement of the M_2S_2 core, with both the metal–metal distance and the M–S–M bridge angle expected to decrease. Published[5,21,26a] X-ray crystallographic studies of $[M_2(CO)_8(SR)_2]^0$ and $[M_2(CO)_8(SR)_2]^{2-}$ complexes, summarized in Table V, are consistent with this interpretation. Each complex is centrosymmetric and possesses a distorted-octahedral geometry around each metal atom. The three M^I_2 complexes have acute M–S–M bridging angles of ca. 74° and short M–M distances of 2.97–2.99 Å, which are consistent with metal-metal bonding. The analogous M(0) dimer, $[Et_4N]_2[Mo_2(CO)_8(SCH_2CO_2Et)_2]$, in which the metal atoms satisfy the 18-electron rule without a metal–metal bond, has a 99° M–S–M bridge angle and a nonbonding M–M distance of 3.94 Å.[26a] Thus, upon oxidation, the metal–metal distance decreases by nearly 1 Å, and the sulfur atoms move 0.6 Å further apart. In addition, the M–S distance is significantly shorter in the M(I) species (2.48 Å) than in the Mo(0) complex (2.59 Å). These structural changes in conjunction with metal–metal bond formation appear to provide the driving force for transfer of two electrons at the same potential. This behavior is analogous to that observed[27] for the phosphido-bridged complexes $Fe_2(CO)_6(PPh_2)_2$ and $[Fe_2(CO)_6(PPh_2)_2]^{2-}$, in which formation and cleavage of a metal–metal bond and structural rearrangement of a bridged dinuclear core also accompany transfer of two electrons.

A final question to consider is the facile nature of the two-electron transfer between $M_2(CO)_8(SR)_2$ and $[M_2(CO)_8(SR)_2]^{2-}$. The current semiclassical theory of electron-transfer reactions[28] considers the activation barrier that controls the rate of such processes to contain contributions from solvent and inner-shell reorganization energies. When large changes in nuclear coordinates accompany charge transfer, the latter term generally becomes predominant and its magnitude is expected to slow the electron-transfer rate. For homogeneous self-exchange reactions of mononuclear transition-metal complexes, significant diminutions in electron-transfer rate constant have been correlated successfully with increased displacements (up to ~0.2 Å) of metal–ligand bond distances.[29] Thus, we find it surprising that the $M_2(CO)_8(SR)_2$ and $[M_2(CO)_8(SR)_2]^{2-}$ complexes, which exhibit large structural differences, should undergo reversible electrode reactions. In Table III the values of ΔE_p at 0.1 V s^{-1} sweep rate are all within a few millivolts of the result $(57/n$ mV) expected for reversible two-electron transfer. Thus, eq 5 exhibits almost fully Nernstian behavior under these conditions.[30] Our explanation is that the molecular motions involved in the interconversion of $M_2(CO)_8(SR)_2$ and $[M_2(CO)_8(SR)_2]^{2-}$ are concerted in such a way that only a low-energy barrier must be crossed despite the large displacements in nuclear coordinates.

There are other instances of essentially reversible, concerted two-electron transfer accompanied by large structural change and metal–metal bond formation that involve binuclear transition-metal complexes, e.g., $[Fe_2(CO)_6(PPh)_2]^{0/2-}$[27] and $[Rh_2(fulvalene)(CO)_2(PR_3)_2]^{0/2+}$,[31] and polynuclear metal clusters, e.g., $[Au_9(PPh_3)_8]^{3+/+}$.[32] These systems apparently profit from similar low-energy pathways for molecular reorganization in conjunction with electron transfer. However, there are structurally similar cases in which concerted two-electron transfer is decidedly irreversible,[33–35] implying larger inner-shell reorganization energy barriers, and still further examples[36,37] in which the multielectron event occurs in a stepwise rather than a concerted fashion. We presume that structural and electronic factors control this range of chemical behavior, but our present understanding of the subject is incomplete.[38]

Acknowledgment. We acknowledge grants from the National Science Foundation (CHE-84-09594 to FAS) and the USDA/SEA Competitive Research Grants Office (85-CRCR-1-1639 to J.W.M. and 81-CRCR-1-0675 to J.W.M. and W.E.N.) for support of this research and thank Professor Fred Anson for enlightening discussions.

(27) (a) Ginsburg, R. E.; Rothrock, R. K.; Finke, R. G.; Collman, J. P.; Dahl, L. F. *J. Am. Chem. Soc.* **1979**, *101*, 6550. (b) Collman, J. P.; Rothrock, R. K.; Finke, R. G.; Moore, E. J.; Rose-Munch, F. *Inorg. Chem.* **1982**, *21*, 146.

(28) Sutin, N. *Prog. Inorg. Chem.* **1983**, *30*, 441.

(29) Brunschwig, B. S.; Creutz, C.; Macartney, D. H.; Sham, T.-K.; Sutin, N. *Faraday Discuss. Chem. Soc.* **1982**, *74*, 113.

(30) Frequent polishing of the glassy-carbon-electrode surface is necessary for obtaining this result. Larger values of ΔE_p are observed at unpolished surfaces or at those that have been in contact with the sample solution for some time, presumably as a result of adsorption. Some data reported in ref 8 and 9 were obtained under such conditions.

(31) (a) Connelly, N. G.; Lucy, A. R.; Payne, J. D.; Galas, A. M. R.; Geiger, W. E. *J. Chem. Soc., Dalton Trans.* **1983**, 1879. (b) Freeman, M. J.; Orpen, A. G.; Connelly, N. G.; Manners, I.; Raven, S. J. *J. Chem. Soc., Dalton Trans.* **1985**, 2283.

(32) (a) van der Linden, J. G. M.; Paulissen, M. L. H.; Schmitz, J. E. J. *J. Am. Chem. Soc.* **1983**, *105*, 1903. (b) van der Velden, J. W. A.; Bour, J. J.; Bosman, W. P.; Noordik, J. H.; Beurskens, P. T. *Recl. Trav. Chim. Pays-Bas* **1984**, *103*, 13.

(33) Rhodes, M. R.; Mann, K. R. *Inorg. Chem.* **1984**, *23*, 2053.

(34) Tulyathan, B.; Geiger, W. E. *J. Am. Chem. Soc.* **1985**, *107*, 5960.

(35) Moulton, R.; Weidman, T. W.; Vollhardt, K. P. C.; Bard, A. J. *Inorg. Chem.* **1986**, *25*, 1846.

(36) Gaudiello, J. C.; Wright, T. C.; Jones, R. A.; Bard, A. J. *J. Am. Chem. Soc.* **1985**, *107*, 888.

(37) McDonald, J. W. *Inorg. Chem.* **1985**, *24*, 1734.

(38) For recent review of the subject of structural change accompanying electron-transfer reactions, see: (a) Geiger, W. E. *Prog. Inorg. Chem.* **1985**, *33*, 275. (b) Geiger, W. E.; Connelly, N. G. *Adv. Organomet. Chem.* **1985**, *24*, 87.